

# The Nuclear Pairing Gap - How Low Can It Go?

B. Alex Brown

*National Superconducting Cyclotron Laboratory and Department of Physics and Astronomy,  
Michigan State University, East Lansing, Michigan 48824-1321, USA*

The pairing gap for  $^{53}\text{Ca}$  obtained from new experimental data on the masses of  $^{52-54}\text{Ca}$  has the smallest value yet observed. This is explained in the framework of the nuclear shell model with schematic and realistic Hamiltonians as being due to shell gaps around the low- $j$  orbital  $1p_{1/2}$ . Minima in the pairing gaps for all nuclei are shown and discussed.

PACS numbers: 21.10.Dr, 21.30.-x, 21.60.Cs

## I. INTRODUCTION

One of the most robust signatures of pairing in nuclei is the odd-even oscillation in the one-neutron separation energies as a function of neutron or proton number. This is illustrated in Fig. 1 which shows the binding energies and one-neutron separation energies for the calcium isotopes. The figure also shows the results of a shell-model calculation in the  $(0f_{7/2}, 0f_{5/2}, 1p_{3/2}, 1p_{1/2})(fp)$  model space with the GX1A Hamiltonian (also referred to as GXPF1A in the literature [1]) compared with experiment. The oscillation in the one-neutron separation energies can be quantified in terms of the energy differences

$$D_n(N) = (-1)^{N+1}[S_n(Z, N+1) - S_n(Z, N)]$$

$$= (-1)^N[2\text{BE}(Z, N) - \text{BE}(Z, N-1) - \text{BE}(Z, N+1)],$$

where  $S_n(N) = \text{BE}(Z, N) - \text{BE}(Z, N-1)$  is the one-neutron separation energy.  $N$  is the number of neutrons and  $Z$  is the number of protons. This quantity turns out to be always positive and reflects the fact that the even nuclei are always more bound on the average than the neighboring odd nuclei. I will distinguish the results for even and odd  $N$  values denoted by,  $D_{ne}$  and  $D_{no}$ , respectively. In the literature one commonly finds the related quantity known as the odd-even mass parameter or pairing gap  $\Delta_n(N) = \frac{D_n(N)}{2}$  (see Fig. 2.5 in [2]). I use  $D$  rather than  $\Delta$  because its values are more directly connected to simple underlying quantities associated with pairing and shell gaps. Equivalent equations as a function of proton number are obtained by fixing  $N$  and varying  $Z$ .

Fig. 2 shows values of  $D_n$  for the calcium isotopes ( $N > 20$ ) obtained from experiment and from two commonly used effective Hamiltonians in the  $fp$  model space, KB3G [3] and GX1A [1] and with a new ab-initio Hamiltonian that includes three-nucleon interactions [4]. I also show the excitation energies for the lowest  $2^+$  states of the even nuclei. The experimental data is from the 2012 mass table [5] together with recent data for  $^{51-54}\text{Ca}$  [6]. The new data provide a point for  $^{53}\text{Ca}$  in the upper panel of Fig. 2 that turns out to be the lowest value for  $D_n$  observed in all nuclei with even  $Z$ . The results are in good

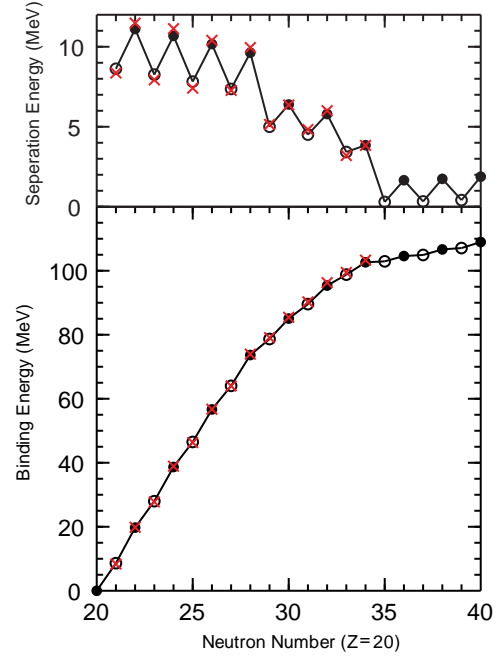


FIG. 1: The bottom panel shows the ground-state energies for the calcium isotopes obtained from the  $pf$  shell-model calculation with the GX1A Hamiltonian relative to  $^{40}\text{Ca}$  with filled circles even  $N$  and open circles for odd  $N$ , all connected by a line. The crosses are the experimental data. The top panel shows the one-neutron separation energies for GX1A and experiment.

agreement with the KB3G and GX1A shell model predictions. In this letter I use the shell model with schematic and realistic Hamiltonians to understand the trends observed for  $D$ , and in particular the low value for  $^{53}\text{Ca}$ . This will be used to qualitatively understand the trends for minima in the  $D$  values for all nuclei.

To obtain insight into the reasons for the patterns observed in Fig. 2, I start with the simple “surface-delta-function” (SDI) model for the interaction [7]. The SDI differs from the delta interaction by the replacement of the radial integrals by a constant. The results for  $D$  obtained with SDI when the single-particle ener-

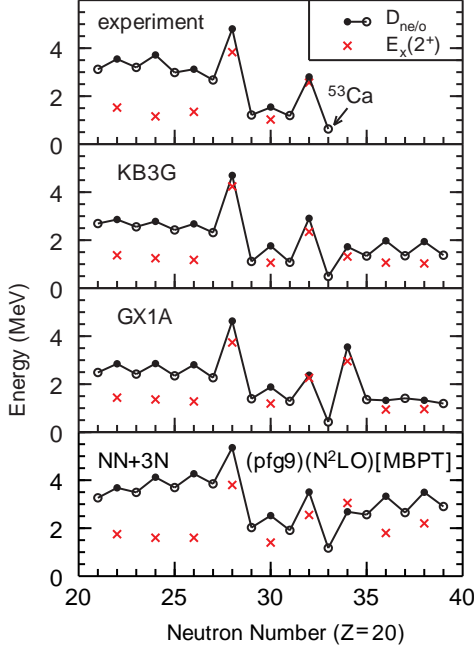


FIG. 2:  $D$  and  $E_x(2^+)$  for the calcium isotopes as a function of neutron number.  $D$  values are shown by the filled circles for even  $N$  and open circles for odd  $N$ , all connected by a line. The  $E_x(2^+)$  values are shown by the crosses.

gies are degenerate are shown in the bottom panel of Fig. 3. The SDI  $J = 0$ ,  $T = 1$  two-body matrix elements for orbitals  $a$  and  $b$  with spins  $j_a$  and  $j_b$  are  $\langle aa | \text{SDI} | bb \rangle = C\sqrt{(2j_a + 1)(2j_b + 1)}$ , where  $C$  is a constant. The interaction strength  $C$  is chosen to give a value for  $D$  that will turn out to be similar to that obtained with the effective  $pf$  shell Hamiltonians for calcium. The excitation energies of the  $2^+$  states are also constant with the SDI and degenerate single-particle energies. The results for  $D$  would be the same if the  $pf$  orbitals were replaced by a single orbital with  $j = 19/2$ , but the constant  $2^+$  energy would be higher (3 MeV). The  $D$  value is determined by the number of  $m$  states that participate in the pairing. The interaction energies obtained with SDI are  $E(n) = \frac{nV_o}{2}$  for even  $n$ , and  $E(n) = \frac{(n-1)V_o}{2}$  for odd  $n$ , and thus  $D = -V_o$ .  $V_o$  is the paired interaction strength for two particles with  $J = 0$ . All of the odd  $N$  nuclei have four degenerate states with  $J^\pi = 1/2^-, 3/2^-, 5/2^-$  and  $7/2^-$ .

Fig. 3 shows the numerical results obtained as the shell gap between the  $0f_{7/2}$  orbital and a degenerate group of  $0f_{5/2}, 1p_{3/2}, 1p_{1/2}$  orbitals is increased from zero to four MeV. The value of  $D_e$  at  $N = 28$  begins to rise when the value of shell gap becomes greater than  $D_o$ . In the infinite gap limit the total original value of 4 MeV is divided between the lower group (1.6 MeV for the  $0f_{7/2}$ ) and the upper group (2.4 MeV for  $0f_{5/2}, 1p_{3/2}, 1p_{1/2}$ ). When the shell gap is well formed the value of  $D$  is nearly equal

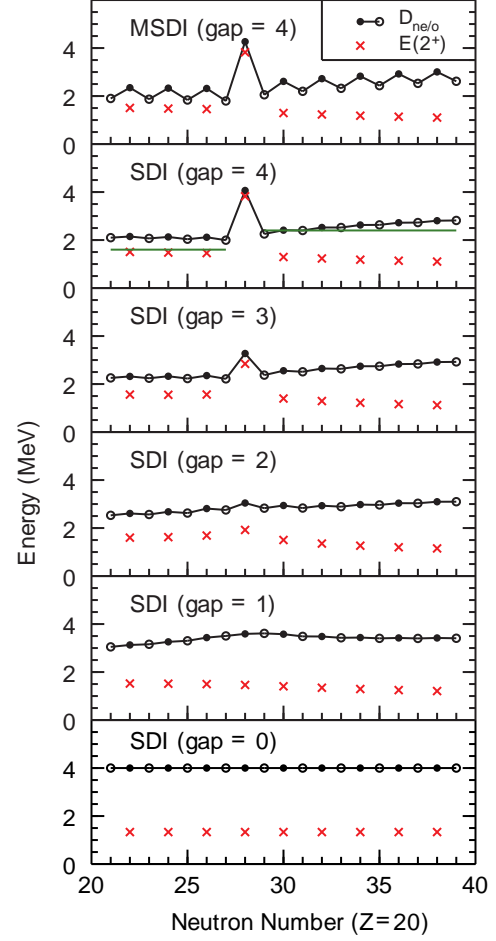


FIG. 3: Results obtained with the SDI interaction as a function of the shell gap between the  $0f_{7/2}$  and  $(0f_{5/2}, 1p_{3/2}, 1p_{1/2})$  set of orbitals. The top panel also show the results for  $D$  (thin lines) obtained when the shell gap is infinite.

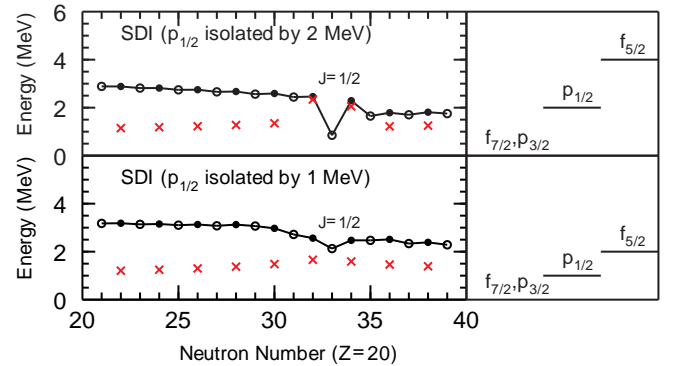


FIG. 4: Results obtained with the SDI interaction as a function of the shell gap between the  $0f_{7/2}$  and  $(0f_{5/2}, 1p_{3/2}, 1p_{1/2})$  set of orbitals. The top panel also show the results for  $D$  (thin lines) obtained when the shell gap is infinite.

to that of the  $2^+$  excitation energy. The experiment and calculations in Fig. 2 show clear signatures of shell gaps at  $N = 28$  and  $N = 32$ . The GX1A calculation also shows a shell gap at  $N = 34$  in contrast to the KB3G and NN+3N models that do not show a gap at  $N = 34$ . Mass measurements for the more neutron-rich calcium isotopes are required for the experimental value at  $N = 34$ . Indirect evidence from production cross section data indicates that the shell gap at  $N = 34$  is about 0.5 MeV smaller than that given by GX1A (and GX1B) [8].

In order to obtain a dip in the  $D_o$  value one needs to make shell gaps below and above a low- $j$  orbital. This is shown in Fig. 4 where there are three groups of orbitals with  $1p_{1/2}$  in the middle split by one and two MeV from the other orbitals. In the limit of a completely isolated  $1p_{1/2}$  orbital  $D_o = -C\sqrt{(2j_a + 1)(2j_b + 1)} = -2C = 0.4$  MeV.

The main defect of the SDI model is the lack of oscillations in the  $D$  values that are observed in experiment. In the 1960's this was recognized as a basic failure of the delta and SDI Hamiltonians. It was empirically fixed by adding a constant to the interaction to make the so-called modified-delta interaction [9] of the form  $V(|\vec{r}_1 - \vec{r}_2|) = A\delta(|\vec{r}_1 - \vec{r}_2|) + B$ . With the SDI form of the radial integral this becomes the so-called modified-surface-delta interaction (MSDI). The modern interpretation of this constant is that it comes from core-polarization corrections and three-body interactions. It is essential to obtain a good saturation property for the binding energies. The  $D$  values obtained with  $B = 0.2$  MeV and with a shell gap of four MeV are shown at the top of Fig. 3. This constant simply adds a term  $n(n-1)B/2$  to the all energies and  $D_o = -V_o - B$  for odd  $n$  and  $D_e = -V_o + B$  for even  $n$ . Half the sum of neighboring even and odd  $D$  gives the pairing contribution:  $D_a = \frac{1}{2}[D_e(N) + D_o(N-1)] = -V_o$ , and half of the difference gives quadratic dependence:  $D_b = \frac{1}{2}[D_e(N) - D_o(N-1)] = B$ . Fig. 2-5 in Bohr and Mottelson [2] is based upon the  $D_a$  combination ( $\Delta = D_a/2$ ).

The Coulomb interaction between protons behaves like the addition of a long-range monopole term in the liquid drop model  $B = (6e^2/5R)$ . There is also a small anti-pairing addition to  $D_a$  of (about +0.10 MeV for  $Z = 20$ ). This is useful for understanding the trends in  $D_p(Z)$  compared to those for  $D_n(N)$ .

Thus, the MSDI model with shell gaps gives a semi-quantitative understanding of all trends observed in  $D_{e/o}$ . The low  $D_o$  value for  $^{53}\text{Ca}$  observed in experiment and theory in Fig. 2 is due to occupation of the  $1p_{1/2}$  orbital at  $N = 33$ . The experimental value for  $^{53}\text{Ca}$  is  $D_o = 0.63(10)$  MeV compared to the calculated values (in MeV) of 1.170 (MBPT), 0.425 (GX1A) and 0.489 (KB3G). The key quantity for the effective Hamiltonians is the  $\langle (1p_{1/2})^2 | V | (1p_{1/2})^2 \rangle$  effective two-body matrix element. It is 0.151 MeV for KB3G and 0.053 MeV for GX1A compared to -0.20 MeV with the MSDI model. If the  $1p_{1/2}$  orbital was completely isolated its  $D_o$  value

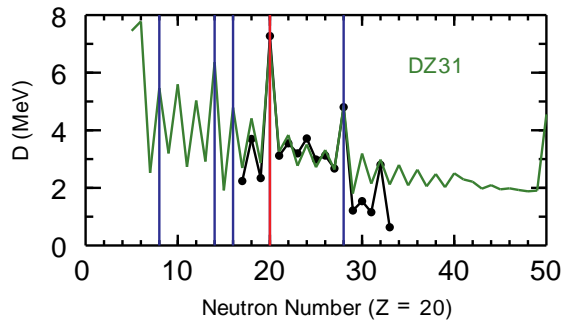


FIG. 5:  $D$  value for the calcium isotopes from experiment (points connected a line) compared to the DZ31 mass model [10] (green line).

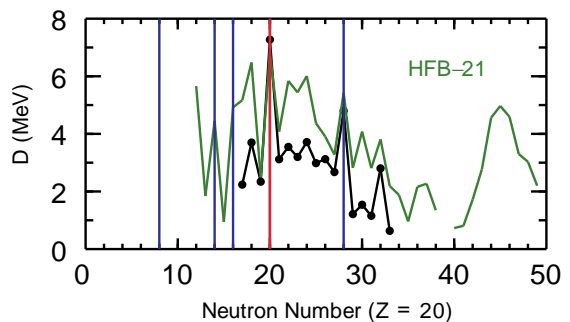


FIG. 6:  $D$  value for the calcium isotopes from experiment (points connected by a line) compared to those obtained with the HFB-21 Skyrme interaction [11] (green line).

would be negative for GX1A and KB3G. The small positive  $D_o$  values obtained with GX1A and KB3G is due to mixing with the other orbitals.

To go beyond the  $pf$  shell we need to consider global mass models such as the 31 parameter model of Duflo and Zuker (DZ31) [10], or the results from more microscopic calculations such as the energy-density functional method with the HFB-21 Skyrme interaction [11]. The DZ31 results shown in Fig. 5 are in rather good agreement with experiment, but it misses the dip at  $N = 33$ . Some parameters of the DZ31 model are determined from this region, but grouping of orbitals considered for the pairing is not correct above  $N = 28$ . The HFB-21 predictions shown in Fig. 6 are rather poor. This could be due to incorrect single-particle energies or an incorrect pairing interaction.

The experimental  $D_{no}$  values for all nuclei obtained from the 2012 mass table [5] and the new calcium experiment [6] are shown in Fig. 7. The value for the  $^{53}\text{Ca}$  at  $N = 33$  is the lowest value obtained for all nuclei and ties with that of  $^{207}\text{Pb}$  that has a value of 0.630. But if one scales residual interaction strength roughly as  $(A)^{-1/2}$ , the scaled minimum is 50% lower in  $^{53}\text{Ca}$  as compared

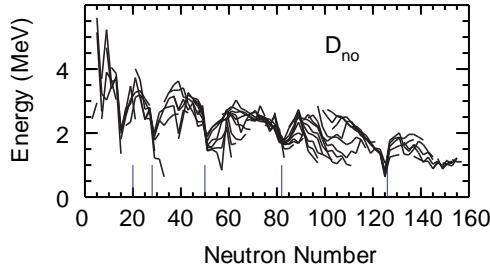


FIG. 7: Experimental values of  $D_{no}$  for all nuclei with even  $Z$ . Values are plotted as a function of the number of neutrons ( $N > Z$ ) and connected by lines for a given  $Z$  value. The vertical lines show the location of the magic numbers 20, 28, 50, 82 and 126.

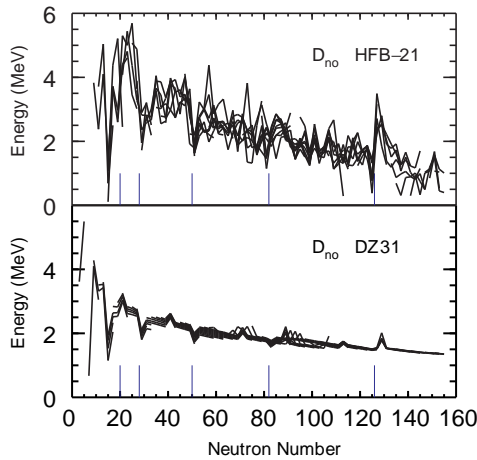


FIG. 8: Theoretical values of  $D_{no}$  for all nuclei with the same range of  $N$  and  $Z$  given by the experimental data in Fig. 7.

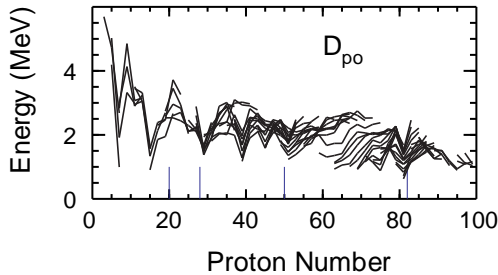


FIG. 9: Experimental values of  $D_{po}$  for all nuclei with even  $N$ . Values are plotted as a function of the number of protons ( $N > Z$ ) and connected by lines for a given  $N$  value. The vertical lines show the location of the magic numbers 20, 28, 50, 82.

to  $^{207}\text{Pb}$ . Another relatively low value occurs for  $N = 57$  at  $^{97}\text{Zr}$  and is associated with a relatively isolated  $2s_{1/2}$  orbital at that point.

The minima at  $N = 33$  is only observed for calcium ( $Z = 20$ ) indicating that required shell gaps quickly disappear. For increasing  $Z$  the  $1p_{1/2}$  and  $0f_{5/2}$  orbitals cross over, and at  $N = 39$  there is a small minimum coming from small gaps around the  $1p_{1/2}$  orbital in  $^{68}\text{Ni}$  ( $Z = 28$ ) and  $^{70}\text{Zn}$  ( $Z = 30$ ). Robust minima are observed for  $N = 15$  due to the  $1s_{1/2}$  orbital and  $N = 127$  due to the  $2p_{1/2}$  orbital. All of these nuclei have a  $J = 1/2$  spin. The  $0d_{5/2} - 1s_{1/2}$  gap disappears for carbon ( $Z = 6$ ) [12], and the  $N = 15$  dip should be gone for  $^{21}\text{C}$ . Mass measurements of  $^{21,22}\text{C}$  are required.

The dip at  $N = 57$  is isolated at  $^{97}\text{Zr}$ . As  $Z$  increases the  $2s_{1/2}$  orbital crosses over the  $0g_{7/2}$  orbital and creates a small dip at  $N = 65$  in  $^{115}\text{Sn}$ . As  $Z$  decreases the  $2s_{1/2}$  orbital should cross over  $1d_{5/2}$  orbital creating a minimum at  $N = 51$  just below  $^{78}\text{Ni}$ . Mass measurements of  $^{78-80}\text{Ni}$  are required.

These experimental trends have been noted previously and compared some HFB models in [13]. The  $D_{no}$  values obtained from the DZ31 and HFB-21 mass models are shown in Fig. 8 where they are plotted for the same range of  $Z$  and  $N$  values known experimentally in Fig. 7. The analytic behaviour of DZ31 is much smoother than experiment. The HFB-21 results are more chaotic than experiment, but show some similarities in the location of the dips to experiment. Neither of these models predicted a dip at  $N = 33$ . The complete set of comparisons experiment for these models is shown on my website [14].

The experimental  $D_{po}$  values for all nuclei obtained from the 2012 mass table [5] are shown in Fig. 9. There are robust minima at  $Z = 7$  (nitrogen) due to the  $0p_{1/2}$  orbital, at  $Z = 15$  (phosphorus) due to the  $1s_{1/2}$  orbital, and at  $Z = 81$  (thallium) due to the  $2s_{1/2}$  orbital. The robust minimum at  $Z = 29$  (copper) is due to the isolated  $1p_{3/2}$  orbital. The minimum at  $Z = 39$  (yttrium) starts at  $N = 38$  and is due to the  $2p_{1/2}$  orbital.  $^{87-97}\text{Y}$  all have  $1/2^-$  ground state spins. Generally the shell gaps are smoothed out by the energy splitting of the Nilsson orbitals in deformed nuclei. But the  $Z = 39$  dip remains in  $^{99-101}\text{Y}$  which are presumably deformed and have uncertain ground-state spins.

In summary, I have shown the oscillations in the neutron separation energy are described by the modified surface delta interaction. In particular the  $D_{no}$  value obtained for  $^{53}\text{Ca}$  is the smallest value yet measured and it due to an isolated  $0p_{1/2}$  orbital. Other mass regions where the effects of isolated low- $j$  orbitals were shown.

**Acknowledgements:** I acknowledge support from NSF grant PHY-1068217.

- (2005).
- [2] A. Bohr and B. R. Mottelson *Nuclear Structure, Vol. I* (World Scientific Publishing Company) (1988).
  - [3] A. Poves, J. Sanchez-Solano, E. Caurier and F. Nowacki, Nucl. Phys. A **694**, 157 (2001).
  - [4] J. D. Holt, T. Otsuka, A. Schwenk and T. Suzuki, Jour. Phys. G **39**, 085111 (2012), and A. Schwenk private communication.
  - [5] M. Wang, G. Audi, A. H. Wapstra, F. G. Kondev, M. MacCormick, X. Xu and B. Pfeiffer, Chinese Physics C **36**, 1603 (2012).
  - [6] F. Wienholtz et al., Nature **346**, 498 (2013).
  - [7] A. Plastino, R. Arvieu and S. A. Moszkowski, Phys. Rev. **145**, 837 (1966).
  - [8] O. B. Tarasov, et al., Phys. Rev. C **87**, 054612 (2013).
  - [9] P. W. M. Glaudemans, P. J. Brussaard and B. H. Wildenthal, Nucl. Phys. **A102**, 593 (1967).
  - [10] J. Dufflo, A. P. Zuker, Phys. Rev. C **52**, 23 (1995); <http://amdc.in2p3.fr/web/dz.html>.
  - [11] S. Goriely, N. Chamel, and J. M. Pearson, Phys. Rev. **82**, 035804 (2010).
  - [12] M. Stanoiu, et al., Phys. Rev. C **78**, 034315 (2008).
  - [13] G. F. Bertsch, C. A. Bertulani, W. Nazarewicz, N. Schunck and M. V. Stoitsov, Phys. Rev. C **79**, 034306 (2009).
  - [14] <http://www.nscl.msu.edu/~brown/resources/resources.html>